Tellus (1986), *38B*, 319–327

Canopy structure and cloud water deposition in subalpine coniferous forests

By GARY M. LOVETT, *Institute of Ecosystem Studies, The New York Botanical Garden, The Mary Flagler Cary Arboretum, Box AB, Millbrook, New York 12545, USA*
and WILLIAM A. REINERS, *Department of Botany, University of Wyoming, Laramie, Wyoming 82071, USA*

(Manuscript received January 9; in final form June 17, 1986)

ABSTRACT

The relationship between canopy structure and cloud water deposition is explored using a modelling approach applied to subalpine conifer forests in the northeastern US. The zero plane displacement height was found to decrease monotonically with stand thinning, while the roughness length showed a unimodal pattern, peaking at a value of total surface area index (SAI) of about 5. The cloud water deposition velocity also was unimodal, increasing from 28 to 34 cm s^{-1} as the simulated stand was thinned from SAI = 13 to SAI = 6, and then decreasing with further thinning. The calculated resistance to cloud water deposition was greater than the resistance to momentum transfer except at very low values of SAI. Evaporation rate also showed a unimodal pattern as a function of SAI, but the pattern was less pronounced than that of cloud water deposition. These results suggest that agents which moderately reduce the SAI of closed forest stands may increase the deposition of cloud water. If some aspect of cloud water deposition causes canopy deterioration in subalpine forests, a positive feedback could occur between the canopy thinning and the cloud water deposition. A calculation of potential deposition on the lee side of gaps in the forest indicates a maximum possible deposition velocity approaching 200 cm s^{-1}, illustrating the expected heterogeneity of deposition rates across the subalpine landscape.

1. Introduction

Cloud water has been shown to be an important carrier for pollutant deposition to high elevation ecosystems (Lovett et al., 1982; Schlesinger and Reiners, 1974; Dollard et al., 1983; Waldman et al., 1985; Scherbatskoy and Bliss, 1983). The incorporation of atmospheric gases and aerosols into cloud droplets, which are typically 5–50 μm diameter, permits the efficient deposition of these substances by droplet sedimentation and impaction if the cloud contacts a vegetation canopy (Lovett, 1984). The key factors controlling the droplet deposition rate are the windspeed, the droplet size distribution, the cloud liquid water content, and the aerodynamic properties of the canopy. Multiplying the droplet deposition rate by the solute concentration yields a deposition rate for the solute. Lovett and Reiners (1983) have shown characteristic solute deposition rates for balsam fir [*Abies balsamea* (L.) Mill] forests of New England mountains to be much higher than would be expected for dry deposition of the particles and gases, and more comparable to rates of deposition by rainfall. Because these ecosystems experience cloud for longer periods than rainfall, the total solute loading via cloud water deposition is greater than the deposition by rainfall. Evaporation from the canopy during cloud deposition events can significantly reduce water deposition, but not chemical deposition, to the forest floor (Lovett et al., 1982). Evaporation from the canopy also increases the chemical concentrations to which the canopy surfaces are exposed (Unsworth, 1985). Even without evaporation, cloud droplets are characteristically highly concentrated in many atmospheric pollutants relative to rainfall (Lovett et al., 1982; Scherbatskoy and Bliss, 1983; Waldman et al., 1982; Dollard et al., 1983; Castillo and Jiusto, 1983). Long periods of cloud immersion in high-elevation forests result in protracted exposure of canopy surfaces to these highly concentrated solutions.

Deposition rates are frequently evaluated by the deposition velocity (v_d) which is the deposition flux (F) of a substance divided by its concentration (C) in the air at some reference height (z):

$$v_d = F/C_z \qquad (1)$$

Theoretical and experimental evidence suggests that the cloud water deposition velocity should be strongly influenced by the aerodynamic properties of the canopy (Lovett and Reiners, 1983; Dollard and Unsworth, 1983). This contrasts with the situation for most gases and small particles, in which canopy aerodynamics exert very little control on deposition velocities (Davidson et al., 1982). In long stretches of uninterrupted forest, cloud droplets reach the canopy surfaces by vertical transport from the air above the canopy. The vertical transport occurs because of turbulence generated at the canopy top. The aerodynamic characteristics of the canopy control the generation of turbulence, and thus regulate the mixing of droplet-laden air to the vicinity of the canopy surfaces. The aerodynamics of the surface also determine in-canopy wind speeds, which in turn control the inertial impaction of droplets through the boundary layers of individual leaves and branches (Thorne et al., 1982).

Most micrometeorological theory and measurements rely on the assumption of a uniform boundary layer over the canopy. Formation of such a boundary layer requires a homogeneous canopy surface, with airflow parallel to the plane of the canopy top for considerable distances upwind of the location of study (Monteith, 1973). These criteria are problematic in many high-elevation forests. In mountainous areas airflow parallel to the canopy surface may be restricted to plateaux or long, constant slopes. In addition, while homogeneous areas of forest do exist at high elevation, many areas are more accurately described as a patchwork of vegetation of varying height, density, and species composition. This mosaic pattern results in part from the severe disturbance regime to which these forests are subjected.

In the Appalachian Mountains of the eastern US, high-elevation vegetation patterns have received considerable study (Sprugel, 1976; Reiners and Lang, 1979; Foster and Reiners, 1983; White et al., 1986). Here, the forest canopy is frequently interrupted by gaps of various sizes caused by windthrow, landslides, insect defoliation, natural regeneration, and other phenomena. The disturbance regime varies with latitude, elevation, and slope aspect, and the gap size created by these disturbances varies from several square meters (the size of a gap left by a single treefall) to thousands of hectares. Infestation of Fraser fir in the southern Appalachians by the balsam woolly adelgid and recent unexplained declines in red spruce in the northern Appalachians present the potential for major shifts in canopy structure over wide areas (Johnson and Siccama, 1983; White et al., 1986).

The purpose of this paper is to point out the relationship between cloud water deposition and canopy structure, and to predict how uniform thinning of a forest canopy will affect the deposition velocity of cloud droplets and the solutes they carry. Because the model used for these predictions is strictly valid only in the case of one-dimensional transport to homogeneous canopies, additional calculations will be made to estimate the magnitude of deposition near gap edges.

2. Deposition model

The cloud water deposition model used in this study is described in detail by Lovett (1984). It was developed, parameterized, and tested in the even-aged, monospecific, balsam fir forests at 1200 m elevation on Mt. Moosilauke, NH, USA (44°01′N, 77°50′W). The model divides the canopy into 1 m height strata, and recognizes seven different canopy components (age and density classes of needles, diameter classes of bare twigs, and trunks) in each stratum. In brief, resistances are used to parameterize transport of droplets between layers and from the air to the canopy surfaces in each layer. Resistances are calculated for each of three size classes of droplets (0–10, 10–20, and 20–30 μm diameter). The between-layer resistances are calculated as the inverse of the turbulent diffusivity integrated over the depth of a canopy stratum. The turbulent diffusivity within the canopy is assumed equal to its canopy-top value (Thom, 1971; Landsberg and Jarvis, 1973), which is calculated from the canopy-top wind speed and the bulk aerodynamic parameters of the canopy as described by Lovett (1984). These calculations involve standard micrometeorological theory (see Thom, 1975) and assume: (1) a homogeneous canopy; (2) neutral stability conditions; and (3) similarity of momentum and cloud droplets with regard to turbulent transport in the canopy. The estimation of canopy aerodynamic parameters from canopy structure data is discussed in section 3 below.

The boundary-layer resistances for the canopy components are calculated from wind tunnel data (Thorne et al., 1982) and are dependent on the wind speed, droplet size and component size. Droplet sedimentation is calculated by applying sedimentation velocities to each droplet size class in each stratum of the canopy. In-canopy wind speeds are calculated to decrease exponentially as a function of the downward-cumulated surface area index (SAI) in the stand and an extinction coefficient measured in the field. Evaporation from the canopy is calculated in a similar fashion, using net radiation and sensible and latent heat exchange in computing the energy balance for each component type in each stratum. Input parameters include meteorological conditions (wind speed, temperature, relative humidity, and net radiation) and cloud characteristics (droplet size distribution and liquid water content) at the canopy top. Testing data included collections of rime ice (frozen cloud water deposition) in a profile in the canopy and measurement of below-canopy drip (throughfall and stemflow) during cloud deposition "events." The model was shown to provide realistic deposition estimates (Lovett, 1984).

3. Canopy structure and aerodynamic parameters

The aerodynamic parameters that govern turbulent transport into plant canopies are the zero plane displacement height (d) and the roughness length (z_0). These are empirical parameters derived from the solution of the steady-state wind profile equation above the canopy, but some attempts have been made to ascertain their physical significance. The zero plane displacement height was determined by Thom (1971) to be the mean level of momentum absorption within the canopy, that is, the mean height of canopy surfaces weighted by their aerodynamic drag. This interpretation has been affirmed experimentally (Landsberg and Jarvis, 1973) and by the modelling analysis of Shaw and Pereira (1982). Thus the zero-plane displacement height can be calculated as:

$$d = \frac{\int_0^h u(z)^{1.5} a(z) z \, dz}{\int_0^h u(z)^{1.5} a(z) \, dz} \tag{2}$$

where $u(z)$ is the wind speed at height z within the canopy, $a(z)$ is the canopy profile of surface area, and h is the height of the canopy. Drag at the forest floor was included in our calculation of d by eq. (2).

The roughness length is associated with the form drag of individual plant crowns, and was suggested by Thom (1971) to be proportional to the difference between the height (h) of the canopy and the displacement height:

$$z_0 = 0.36(h - d). \tag{3}$$

However, both experimental and theoretical evidence suggest that z_0 should be a nonlinear function of (h–d) as canopy structure changes (Raupach et al., 1979; Shaw and Pereira, 1982; Seginer, 1974). Lettau (1969) suggested that z_0 should be related to the size and density of the roughness elements, and derived the following equation for solid roughness elements:

$$z_0 = C_d h_e S N / A \tag{4}$$

where C_d is a drag coefficient for an individual roughness element, h_e is the effective height of the roughness elements, S is their silhouette area normal to the direction of the wind flow, and N is the number of roughness elements in area A. Lettau (1969) found eq. (4) to predict z_0 quite well for solid roughness elements, but Leonard and Federer (1973) had less success in applying this formulation to a pine canopy by considering individual tree crowns to be the roughness elements.

Eq. (4) can be modified to be appropriate for porous canopies by taking account of the fact that momentum is absorbed by individual leaves, shoots, and branches rather than by whole tree crowns. If we assume that only those canopy elements above the zero plane are effective in generating turbulence, the effective height h_e can be considered to be $(h - d)$. The drag coefficient is chosen to be an average value appropriate for individual leaves or branches above the zero plane in a canopy. The terms SN/A in eq. (4) represent the surface area contributing to the roughness, divided by the ground area. For porous canopies, this is simply the plant surface area index above the zero plane, here termed A_d. Thus eq. (4), when modified for vegetation canopies, becomes:

$$z_0 = C_d(h - d)A_d. \tag{5}$$

We used this formulation for z_0 in this study. The behavior of the equation and support for its accuracy are discussed below. We chose 1.0 to be an appropriate drag coefficient for spruce and fir needles, using total needle area as a basis to be consistent with our specification of A_d.

4. Modelling experiments

For the first set of simulations reported below, we used as a starting point the vertical distribution of plant surface area as shown in curve A of Fig. 1. This surface area profile was calculated by regression equations based on the results of destructive sampling of balsam fir trees near our study area (Lovett, 1981). In two simulation experiments, the canopy structure was altered by eliminating 0–2 yr old needles or >2 yr old needles, resulting in the surface area profiles shown in curves C and B, respectively, of Fig. 1. The height of the stand remained constant at 10.6 m (height of tallest tree). Eqs. (2) and (5) were used to calculate d and z_0 for these stands, and the cloud water deposition/evaporation model was used to predict the cloud water deposition velocity and water flux rates for droplet deposition and evaporation.

In the second set of experiments, the SAI profile in Fig. 1, curve A was taken as a standard, and the SAI value was varied continuously in the range of 1–13 $m^2\ m^{-2}$ by reducing all foliage

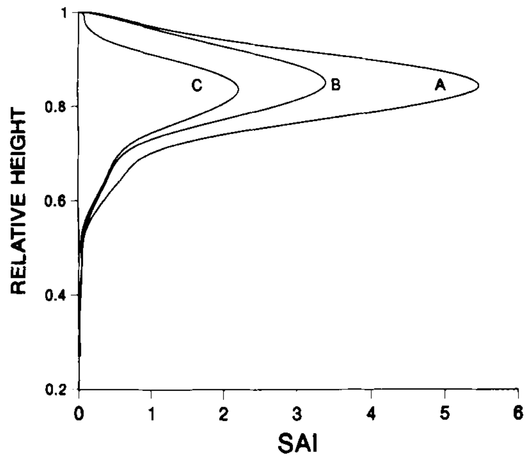

Fig. 1. Profiles of surface area index (SAI) for three stands. A: normal canopy structure, B: needles >2 yrs old eliminated, C: needles 0–2 yrs old eliminated. Surface area expressed as SAI per 1 m height stratum.

types equally. Thus the proportion and distribution of the different foliar types remained constant, while the actual SAI varied. Calculations of d, z_0, cloud water deposition, and evaporation were made as above. For all simulations, the following canopy-top conditions were assumed: wind speed = 4 m s^{-1}, temperature = 10°C, relative humidity = 98%, net radiation = 0, and cloud liquid water content = 0.4 g m^{-3}. We used a droplet size distribution described by Best (1951) with a modal size of 10 μm.

5. Results and discussion

Table 1 shows the results of the first set of computational experiments, in which a "standard" SAI profile (Fig. 1, curve A) was altered by elimination of > 2 yr old needles (curve B) or 0–2 yr old needles (curve C). Elimination of the young needles had a greater effect on total SAI than did elimination of the older needles, so that the order of the simulated stands with respect to SAI was A > B > C. The zero plane displacement height (d) was decreased as the canopy lost needles, because the center of action of the drag force for the stand decreased as the foliage near the top of the canopy was reduced.

Table 1. *Stand surface area index (SAI), aerodynamic parameters, and cloud water deposition velocities for three balsam fir stands with different canopy structure treatments as shown in Fig. 1. For all simulations, $u_h = 4$ m s^{-1} and mode of drop diameter distribution = 10 µm*

Stand	A	B	C
Treatment	none	eliminate needles >2 yrs old	eliminate needles 0–2 yrs old
SAI	11.3	7.5	4.4
z_0 (cm)	46	67	80
d (cm)	927	890	807
v_d (cm s^{-1})	29	34	31

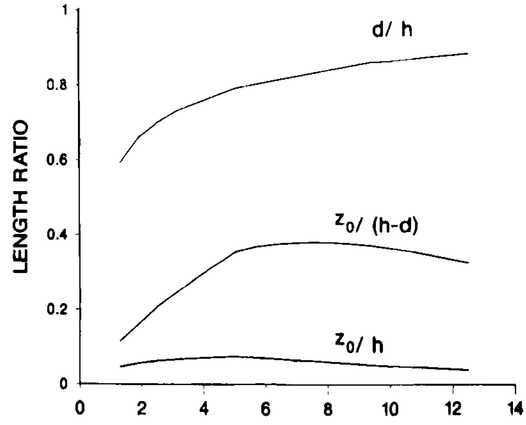

Fig. 2. Canopy aerodynamic parameters versus SAI.

The order of stands with respect to d was the same as for SAI, i.e., A > B > C. The roughness length (z_0) as calculated from eq. (5) is proportional to $(h-d)$, so as d decreases z_0 increases, since h is held constant. The order of stands with respect to z_0 is therefore reversed: C > B > A.

The deposition velocity for cloud water is influenced by canopy roughness, and responds to the treatments shown in Table 1. The simulated deposition velocities for the three stands are in the order B > C > A, which is different from the order of any of the above parameters. It is difficult to interpret the effect of canopy structure on deposition from these data because two aspects of canopy structure are changing simultaneously—total SAI and proportions of the various foliar age classes. For this reason we attempted the next set of simulations in whcih the total SAI varied but the relative proportions of foliage types remained constant. We will proceed now with analysis of those results, and return later to Table 1.

Fig. 2 shows the variation in d and z_0 (expressed as fractions of the canopy height h for comparison with other studies) over the range of SAI of approximately 1–13 m^2 m^{-2} (surface area of all sides of canopy components). Actual SAI values for subalpine forests vary widely, but for dense fir canopies, values in the range 10–12 are typical (Foster, 1984). The relative height distribution of foliage in these simulated stands is that shown in Fig. 1, curve A. As the canopy is thinned homogeneously (i.e., reading from right to left on Fig. 2), our model predicts that d/h will decrease monotonically but not linearly and z_0/h will increase initially and then decrease, peaking around SAI = 5. The ratio $z_0/(h-d)$ is also unimodal, reaching a maximum value of about 0.38 with SAI in the range of 6–8. This curve shape is consistent with the wind tunnel experiments of Raupach et al. (1979) and the theoretical studies of Seginer (1974) and Shaw and Pereira (1982). These studies used quite different means of arriving at conclusions about z_0 than did the present study. Fig. 2 shows that at high SAI values $z_0/(h-d)$ is relatively constant in the range 0.32–0.36, which is close to the mean value calculable from the data of Jarvis et al. (1976) for 13 conifer forests (mean = 0.31, s.d. = 0.14). Thus the rather simple formulation for z_0 in eq. (5) appears to be supported by the limited data available. Note that the formulation by Thom (1971), as shown in eq. (3), predicts the ratio $z_0/(h-d)$ to be constant at 0.36; we believe this to be an overly simplified treatment.

Using these aerodynamic parameters in the cloud deposition model, we can predict the cloud water deposition velocity (v_d), which is shown in Fig. 3 as a function of SAI. The deposition velocity increases as the canopy is thinned below SAI = 13, peaking at a value of v_d = 34 cm s^{-1} at SAI = 6. This represents a 24% increase over the v_d for a stand of SAI = 12.5. With thinning below SAI = 6, v_d decreases. If eq. (3) is used instead of eq. (5) to predict the roughness length, z_0 increases monotonically as the canopy thins, but

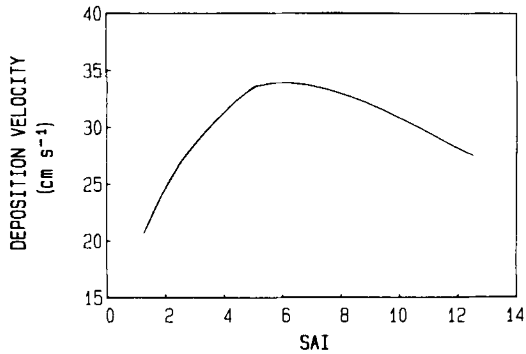

Fig. 3. Simulated deposition velocities for cloud water versus SAI.

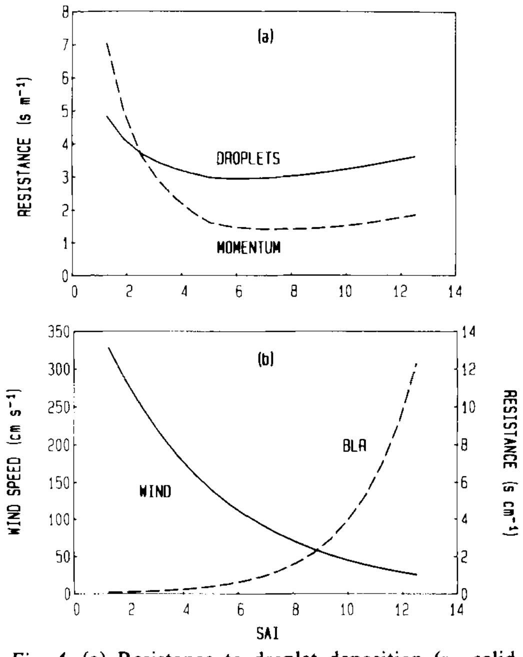

Fig. 4. (a) Resistance to droplet deposition (r_d, solid line) and momentum transfer (r_m, dashed line) versus SAI. (b) Wind speed at 8 m in the canopy (solid line, left scale) and representative boundary-layer resistance (BLR, dashed line, right scale) for a 10 μm droplet at the corresponding wind speed. Values of BLR calculated from wind tunnel data (Thorne et al., 1982) on isolated balsam fir shoots.

the deposition velocity still shows the unimodal pattern. Thus the qualitative results shown in Fig. 3 appear to be independent of the exact specification of z_0.

The behavior of v_d in response to canopy thinning is intriguing, and deserves elaboration. The total resistance to droplet deposition ($r_d = v_d^{-1}$) is plotted vs SAI in Fig. 4a. Also shown in Fig. 4a is the resistance to momentum transport ($r_m = u_h/u_*^2$, where u_h is the wind speed at the canopy top and u_* is the friction velocity) for the simulated canopies. We show r_m here because it is frequently used as an indicator of the "aerodynamic" resistance to mass transport to plant canopies. The aerodynamic resistance is often conceived as acting in series with one or more "surface" or "canopy" resistances, summing to a total resistance to deposition (see Fowler, 1980, for a general treatment, or Shuttleworth, 1977, for the case of fog droplets).

For canopies with high SAI, r_m is about half of r_d (Fig. 4a). Below SAI = 5, r_m increases rapidly, corresponding to the decrease in $z_0/(h-d)$ shown in Fig. 2, and suggesting a decrease in the efficiency of turbulent mixing into the canopy. The convergence of r_m and r_d at low SAI indicates that the "canopy" resistance becomes negligible. This occurs because, as the canopy is thinned, wind speeds within the canopy increase and droplet impaction onto canopy surfaces becomes more efficient. These points are illustrated in Fig. 4b, in which the wind speed at 8 m (= 0.75 h, chosen arbitrarily as representative of the foliated region) in the canopy is plotted vs SAI. (Recall that wind speeds are calculated to decrease exponentially within the canopy as a function of downward-cumulated SAI, and that the canopy-top wind speed is held constant at 400 cm s^{-1} for these simulations.) Also plotted in Fig. 4b is the resistance to impaction of a 10 μm droplet on an isolated balsam fir shoot at the wind speed indicated for the 8 m height. These resistances were calculated from the wind-tunnel data of Thorne et al. (1982), and we show them as an example of the decrease in boundary-layer resistances throughout the canopy in response to thinning.

The common assumption that r_m is a minimum resistance for the transfer of mass to a canopy appears to be inappropriate for the very porous canopies corresponding to the lowest SAI values in Fig. 4a. In these canopies, r_d is less than r_m for two reasons. First, our model includes droplet sedimentation in the calculation of deposition, and thus of r_d. Sedimentation can enhance the deposition of droplets at low SAI, despite the increase in r_m. Second, r_m includes both aerodynamic and boundary-layer components of momentum transfer. It is used as an approximate indicator of aerodynamic resistances to mass transfer because the boundary-layer resistance for momentum transfer is usually assumed to be negligible compared to that for most particles and gases. This is a poor assumption in the case of cloud droplets, however, because wind tunnel studies have shown that impaction of droplets can be more efficient than momentum transfer through the boundary layer, especially at high wind speeds (Chamberlain, 1975). If the true "aerodynamic" resistances for droplets and momentum are equal, then the total resistance to droplet transfer (r_d) can be less than the total resistance to momentum transfer (r_m).

We caution that neither the droplet deposition nor momentum transfer aspects of this model have been tested in real forests of very low SAI, so these results must be interpreted judiciously. Nevertheless, the possibility that r_m may not be a minimum resistance for droplet deposition has been suggested by several experimental studies. Dollard and Unsworth (1983) found that the efficiency of fog droplet deposition (as measured by a micrometeorological technique) could exceed that for momentum in a grass canopy, and Chamberlain (1975) summarized data leading to the same conclusion for an isolated spruce tree.

Fig. 5 illustrates the trends of cloud water

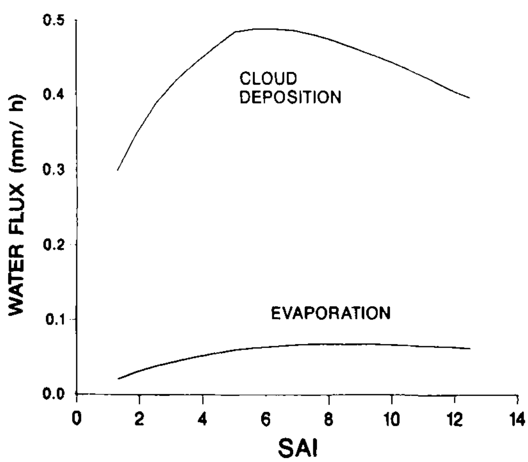

Fig. 5. Simulated water fluxes from cloud water deposition and evaporation versus SAI.

deposition and evaporation flux as functions of SAI. Evaporation is nearly constant at high SAI values but decreases with severe thinning. Increases in evaporation are not sufficient to counterbalance increases in cloud water deposition as the canopy is thinned from SAI = 13 to SAI = 5, so net cloud deposition (the difference between gross cloud deposition and evaporation) will show nearly the same unimodal pattern as does gross cloud deposition. It should be noted that chemical deposition to these forests is related to gross, not net, cloud deposition. Fig. 5 suggests that the evaporative concentration of the solution on canopy surfaces during periods of cloud immersion would be less pronounced in a moderately thinned stand because the ratio of cloud deposition to evaporation increases with moderate thinning.

By comparing Fig. 3 and Table 1, one can see that the deposition velocities for the three stands in Table 1 are not very different from those given in Fig. 3 for stands with corresponding values of SAI. In Table 1, therefore, it appears that the primary canopy structure characteristic influencing the predicted deposition velocity is the quantity of SAI eliminated rather than the age of the lost foliage or its vertical position in the canopy. Comparison with Fig. 3 indicates that stands A and B are in a region where further thinning will increase the deposition velocity while in stand C, further thinning will decrease the deposition velocity. Our canopy sampling data do not permit resolution of smaller age classes of foliage, but with SAI profiles weighted to the top as much as those of these subalpine forests (Fig. 1), manipulating smaller age classes would be unlikely to produce any major effects on the overall SAI profile of the stand.

Our simulations indicate that reductions in canopy surface area applied homogeneously to all trees in a closed balsam fir forest will initially increase the deposition rate of cloud water. If pollutants carried in cloud water somehow contribute to the high-elevation canopy dieback that is currently being observed in the eastern US, then the potential exists for a positive feedback relationship in which initial foliar loss promotes greater deposition which promotes greater foliar loss, etc. This would be a self-limiting process, however, in that SAI would eventually decrease to a level that caused decreased cloud water deposition. Other disturbances which tend to thin the canopy gradually, like low-level insect attack, ozone damage, and breakage of shoots by wind or ice would also cause increases in cloud water deposition.

Because the SAI totals and height profiles for these forests are not radically different from those of other closed, even-aged coniferous canopies (e.g., Kinerson and Fritschen, 1971; Landsberg and Jarvis, 1973), we expect these results to be applicable to other natural or managed conifer forests.

It is frequently the case that canopies do not thin homogeneously but rather that gaps open in the forest from the total defoliation of several trees in the same area. The effect of gaps on the deposition to neighboring trees is difficult to determine because understanding airflow over heterogeneous surfaces is a formidable problem both experimentally and theoretically. In general, however, one would expect increased penetration of canopy-top air into the gap, resulting in higher deposition rates to the forest edge downwind of the gap. A maximum estimate of deposition in this case can be made by assuming that all foliage on the downwind edge of the gap is exposed to the wind speed and cloud liquid water content characteristic of the air above the adjacent homogeneous canopy. Using a wind speed of 4 m s^{-1}, a droplet size of 10 μm, a leaf area index of 12, and droplet capture efficiencies for needles as determined by Thorne et al. (1982), we calculate a deposition velocity of about 200 cm s^{-1} at the gap edge. This is about seven times greater than the deposition velocity expected under similar conditions in a closed canopy (Fig. 3), but we emphasize that this is a maximum possible value for the specified conditions. Because both wind speed and liquid water content decline exponentially with depth in the canopy in the case of vertical transport (Lovett, 1984), we expect that deposition rates will decline exponentially with distance downwind from a gap edge until reaching a value characteristic of the closed canopy. While the trees on the downwind edge of the gap would experience higher deposition locally, the effect of a gap on the deposition to the forest landscape as a whole may not be increased, since the open area of the gap itself would probably experience lower deposition rates than the surrounding forest. The effects of gaps on deposition to an entire landscape would be a complex function of gap size and frequency.

6. Conclusions

The computational experiments of this study have generated a number of predictions regarding the effect of canopy structure on cloud water deposition. These predictions are stated below as hypotheses to be tested by future work in the field.

(1) Homogeneous thinning of a closed coniferous forest will result in increased cloud water deposition until the total SAI drops below a critical value in the range of 5–6 m^2 m^{-2}.

(2) Thinning of stands below this critical SAI will result in decreased cloud water deposition.

(3) In severely thinned stands, efficiency of droplet deposition will exceed that of momentum.

(4) The unimodal pattern of deposition velocity in response to thinning will apply despite differences in the age of the foliage lost.

(5) Canopy disturbance producing significant gaps in the forest will cause large increases in deposition rates locally on the downwind sides of the gaps. This enhancement of deposition will decrease exponentially with distance downwind of the edge of the undisturbed forest.

7. Acknowledgements

This work was supported by the Electric Power Research Institute (RP 1907-1 and RP 2621 to Oak Ridge National Laboratory) and by the US National Science Foundation (Grant DEB 79-07346 to Dartmouth College). This is a contribution to the program of the Institute of Ecosystem Studies, The New York Botanical Garden.

REFERENCES

Best, A. C. 1951. Drop-size distribution in cloud and fog. *Q. J. R. Meteorol. Soc. 77*, 418–426.

Castillo, R. A. and Jiusto, J. E. 1983. Characteristics of nonprecipitating stratiform clouds. In: *Precipitation*

Scavenging, Dry Deposition, and Resuspension (eds. H. R. Pruppacher, R. G. Semonin and W. G. N. Slinn). New York: Elsevier, 15–124.

Chamberlain, A. C. 1975. The movement of particles in plant communities. In: *Vegetation and the Atmosphere*. Vol. I: Principles (ed. J. L. Monteith). New York: Academic Press, 155–203.

Davidson, C. I., Miller, J. L. and Pleskow, M. A. 1982. The influence of surface structure on predicted particle dry deposition to natural grass canopies. *Water, Air, and Soil Pollut. 18*, 25–43.

Dollard, G. J. and Unsworth, M. H. 1983. Field measurements of turbulent fluxes of wind-driven fog drops to a grass surface. *Atmos. Environ. 17*, 775–780.

Dollard, G. J., Unsworth, M. H. and Harve, M. J. 1983. Pollutant transfer in upland regions by occult precipitation. *Nature 302*, 241–243.

Foster, J. R. 1984. Causes of tree mortality in wave-regenerated balsam fir forests. Ph.D. Thesis, Dartmouth College, Hanover, NH, USA.

Foster, J. R. and Reiners, W. A. 1983. Vegetation patterns in a virgin subalpine forest at Crawford Notch, White Mountains, New Hampshire. *Bull. Torrey Bot. Club 110*, 141–153.

Fowler, D. 1980. Removal of sulphur and nitrogen compounds from the air in rain and by dry deposition. In: *Ecological Impacts of Acid Precipitation* (eds. D. Drabløs and A. Tollan), Oslo: SNSF, 22–32.

Jarvis, P. G., James, G. B. and Landsberg, J. J. 1976. Coniferous forests. In: *Vegetation and the Atmosphere, Vol. 2* (ed. J. L. Monteith). London: Academic Press, Inc., 171–240.

Johnson, A. H. and Siccama, T. G. 1983. Acid deposition and forest decline. *Environ. Sci. Technol. 17*, 294A–305A.

Kinerson, R., Jr. and Fritschen, L. J. 1971. Modelling a coniferous forest canopy. *Agric. Meteorol. 8*, 439–445.

Landsberg, J. J. and Jarvis, P. G. 1973. A numerical investigation of the momentum balance of a spruce forest. *J. Appl. Ecol. 10*, 645–655.

Leonard, R. E. and Federer, C. A. 1973. Estimated and measured roughness parameters for a pine forest. *J. Appl. Meteorol. 12*, 302–307.

Lettau, H. 1969. Note on aerodynamic roughness-parameter estimation on the basis of roughness-element description. *J. Appl. Meteorol. 8*, 828–832.

Lovett, G. M. 1981. Forest structure and atmospheric interactions: predictive models for subalpine balsam fir forests. Ph.D. Thesis, Dartmouth College, Hanover, NH, USA.

Lovett, G. M. 1984. Rates and mechanisms of cloud water deposition to a subalpine balsam fir forest. *Atmos. Environ. 18*, 361–371.

Lovett, G. M. and Reiners, W. A. 1983. Cloud water: an important vector of atmospheric deposition. In: *Precipitation Scavenging, Dry Deposition, and Resuspension* (eds. H. R. Pruppacher, R. G. Semonin and W. G. N. Slinn). New York: Elsevier, Inc., 171–180.

Lovett, G. M., Reiners, W. A. and Olson, R. K. 1982. Cloud droplet deposition in subalpine balsam fir forests: hydrological and chemical inputs. *Science 218*, 1303–1304.

Monteith, J. L. 1973. *Principles of Environmental Physics*. London: Edward Arnold.

Raupach, M. R., Thom, A. S. and Edwards, I. 1979. A wind-tunnel study of turbulent flow close to regularly-arrayed rough surfaces. *Boundary-Layer Meteorol. 18*, 373–397.

Reiners, W. A. and Lang, G. E. 1979. Vegetational patterns and processes in the balsam fir zone, White Mountains, New Hampshire. *Ecology 60*, 403–417.

Scherbatskoy, T. and Bliss, M. 1983. Occurrence of acidic rain and cloud water in high elevation ecosystems in the Green Mountains of Vermont. In: *The Meteorology of Acidic Deposition*. Pittsburg, Pennsylvania: Air Pollution Control Association.

Schlesinger, W. H. and Reiners, W. A. 1974. Deposition of water and cations on artificial foliar collectors in fir krummholz of New England Mountains. *Ecology 55*, 378–386.

Seginer, I. 1974. Aerodynamic roughness of vegetated surfaces. *Boundary-Layer Meteorol. 5*, 383–393.

Shaw, R. H. and Pereira, A. R. 1982. Aerodynamic roughness of a plant canopy: a numerical experiment. *Agric. Meteorol. 26*, 51–65.

Shuttleworth, W. J. 1977. The exchange of wind-driven fog and mist between vegetation and the atmosphere. *Boundary-Layer Meteorol. 12*, 463–484.

Sprugel, D. G. 1976. Dynamic structure of wave-regenerated *Abies balsamea* forests in the north-eastern United States. *J. Ecol. 64*, 889–911.

Thom, A. S. 1971. Momentum absorption by vegetation. *Q. J. R. Meteorol. Soc. 97*, 414–428.

Thom, A. S. 1975. Momentum, mass, and heat exchange of plant communities. In: *Vegetation and the Atmosphere. Vol. I: Principles* (ed. J. L. Monteith). New York: Academic Press, 57–109.

Thorne, P. G., Lovett, G. M. and Reiners, W. A. 1982. Experimental determination of droplet impaction on canopy components of balsam fir. *J. Appl. Meteorol. 21*, 1413–1416.

Unsworth, M. H. 1985. Evaporation from forests in cloud enhances the effects of acid deposition. *Nature 312*, 262–264.

Waldman, J. M., Munger, J. W., Jacob, D. J., Flagan, R. C., Morgan, J. J. and Hoffman, M. R. 1982. Chemical composition of acid fog. *Science 218*, 677–680.

Waldman, J. M., Munger, J. W., Jacob, D. J. and Hoffman, M. R. 1985. Chemical characterization of stratus cloudwater and its role as a vector for pollutant deposition in a Los Angeles pine forest. *Tellus 37B*, 91–108.

White, P. S., MacKenzie, M. D. and Busing, R. T. 1986. Natural disturbance and gap-phase dynamics in southern Appalachian spruce-fir forests, USA. *Can. J. For. Res.*, in press.